RSC Advances

PAPER

View Article Online
View Journal | View Issue

Cite this: *RSC Adv.*, 2025, **15**, 5124

Synthesis, characterization, and biomedical applications (antibacterial, antibiofilm, anticancer and effects on hospital-acquired pneumonia infection) of copper titanium oxide nanostructures

Mohsen Poudineh,[ab] Movlud Valian,[c] Amar Yasser Jassim,[d] Zahra Ghorbani,[ab] Azad Khaledi*[ab] and Masoud Salavati-Niasari *[c]

Hospital-acquired pneumonia (HAP) is the second most common cause of nosocomial infections and is responsible for 15% of nosocomial infections, with a high mortality rate, which has led to increased concern and significant costs in healthcare settings. The most significant agents of HAP are *Pseudomonas aeruginosa* and *Klebsiella pneumoniae*, which create a biofilm that results in a resistant infection. We aimed to study the synthesis of $Cu_2Ti_2O_5$ nanoparticles, their effects on the growth and biofilms of *Pseudomonas aeruginosa* and *Klebsiella pneumoniae* isolated from respiratory infections, and their anticancer effects. In this study, for the first time, the Pechini method was used to synthesize $Cu_2Ti_2O_5$ nanostructures. The effects of nanoparticles on the growth and biofilms of *Pseudomonas aeruginosa* and *Klebsiella pneumoniae* were evaluated using a microdilution broth and the microtiter plate method, and the cytotoxic effect of the nanoparticles on the A549 cell line was also assessed by MTT. The characteristics of the nanoparticles were confirmed through XRD, FTIR, SEM, and TEM techniques. $Cu_2Ti_2O_5$ showed a minimum inhibitory effect in concentrations of 156.25 to 625 μg mL^{-1} for ten isolates of *K. pneumoniae* and 625 to 1250 μg mL^{-1} for ten isolates of *P. aeruginosa* and at sub-MIC concentrations as well. It reduced the biofilms of *K. pneumoniae* and *P. aeruginosa* strains by 75% and 44.4%. The nanoparticles killed 50% of A549 cancer cells in 48 h at concentrations of 30 to 40 μg mL^{-1} and in 24 h at concentrations of 200 to 250 μg mL^{-1}. The findings of this study show the antibacterial, anti-biofilm, and anti-cancer effects of $Cu_2Ti_2O_5$ nanoparticles. Therefore, these nanoparticles can be considered potential antimicrobial candidates; however, these effects should be confirmed with more bacterial isolates.

Received 1st December 2024
Accepted 10th January 2025

DOI: 10.1039/d4ra08476d

rsc.li/rsc-advances

1. Introduction

Hospital-acquired infections (nosocomial infections) are challenging complications that require serious attention worldwide. The term refers to infections that the patient has not received before hospital admission. Hospital-acquired infections (HAI) occur in the first moments of a patient's presence in a hospital or within 48–72 h after admission. These days, these infections are of notable concern for medical organizations, leading to an increase in the duration of treatment and significant global costs in healthcare, thus by lowering hospital-acquired infections, there will be noticeable savings in different costs of healthcare systems and treatment.[1] Approximately 75% of the HAI burden is on people who live in developing countries.[2]

Hospital-acquired pneumonia (HAP) occurs in 0.5–1.5% of hospitalized patients. It is the most common cause of death among hospital-acquired infections.[3] HAP is defined as pneumonia that happens 48 h or more after reception of the patient, which was not incubated at the time of admission[4] Up to 6.8% of patients who were admitted to intensive care units (ICUs) were exposed to nosocomial pneumonia. Several pathogens have been proven to be the cause of pneumonia in hospitalized patients.[5]

A set of six organisms (*Staphylococcus aureus*, *P. aeruginosa*, *Klebsiella* species, *Escherichia coli*, *Acinetobacter* species, and *Enterobacter* species) cause almost 80% of hospital-acquired pneumonia episodes.[6] *P. aeruginosa* is an opportunistic bacterium that can cause infections from mild to severe, which are a threat to life. It is known as a cause of hospital-acquired infections. The eradication of *P. aeruginosa* is challenging because of its different resistance mechanisms, such as low

[a]*Infectious Diseases Research Center, Kashan University of Medical Sciences, Kashan, Iran. E-mail: azadkh99@gmail.com; Fax: +98 315 5913201; Tel: +98 315 5912383*
[b]*Department of Microbiology and Immunology, Faculty of Medicine, Kashan University of Medical Sciences, Kashan, Iran*
[c]*Institute of Nano Science and Nano Technology, University of Kashan, P. O. Box 87317-51167, Kashan, Islamic Republic of Iran. E-mail: salavati@kashanu.ac.ir*
[d]*Department of Marine Vertebrates, Marine Science Center, University of Basrah, Iraq*

outer membrane permeability, efflux mechanisms, mutations in genes targeted by antibiotics, biofilm formation, and various virulence factors.[7] It is one of the most common pathogens in hospitals due to innate resistance against different antibiotics and antiseptics, and its ability to live in humid and biofilm-forming conditions. *P. aeruginosa* associated HAP mortality is the highest owing to the high pathogenicity of *P. aeruginosa*, as well as the administration of unsuitable antibiotic therapies for MDR isolates.[8]

Klebsiella pneumoniae is one of the most threatening pathogens for healthcare systems that can cause HAI.[9,10] *K. pneumoniae* through different virulence factors, such as fimbria types 1 and 3, lipopolysaccharides and its outer cell membrane, can escape from the host immune system and produce a biofilm. Due to the increasing spread of multi-drug resistant (MDR) strains of this microorganism and fewer treatment options, it has become a serious threat.[9,11]

Biofilm-related infections are more common in hospital environments due to their rebellious existence and difficulty in treatment. It is estimated that biofilms cause more than 65% of hospital-acquired infections, about 80% of chronic infections, and 60% of all human bacterial infections.[12] Biofilm-related infections cause an increase in patient mortality, prolonged stay in hospitals, and high costs. Gram-positive and Gram-negative microorganisms can both cause HAP. Among them, *P. aeruginosa* and *K. pneumoniae* can produce more biofilm than other biofilm-producers.[12–16]

The strong emergence of multidrug resistance pathogens shows a need for an improvement in new alternative treatment methods. One of those methods is the use of nanoscale materials.[17] These nanoparticles can be used as antimicrobial agents due to their ability to penetrate bacterial membranes and disrupt biofilms.[18] Because of their selectivity and ability to succeed in biological and pharmaceutical uses, metallic nanoparticles have gained a lot of attention. Most metal oxide nanoparticles, such as TiO_2, ZnO, MgO, CuO, SiO_2, and CoO, have demonstrated good antimicrobial properties.[19]

Nanoparticles are promising tools for dealing with biofilms because pathogens with antibiotic resistance mechanisms cannot be resistant to nanoparticles.[20] Until now, several nanoparticles have shown a greater antibiofilm effect than classic antibiotics.[21] For a nanoparticle to be considered a good antimicrobial agent, it must have the ability to bind, inhibit, or slow down the growth of microorganisms. Binding happens because of a positive zeta potential that can improve the interaction between nanoparticles and the pathogen's cell membrane. This interaction can destroy the cell membrane and decrease vitality or cause greater penetration. The antimicrobial activity of nanoparticles is related to their size, form, and charge.[22]

Titanium dioxide is a metallic nanoparticle with strong photolytic capability for environmental cleaning and disinfecting, with different functions in medical and biological fields, like drug and gene transfer.[23] Titanium dioxide nanoparticles show good antimicrobial and antibiofilm activity, because of their stability and size. These functions happen because of their ability to go through the bacterial cell wall and interact with the cell membrane.[24]

Copper oxide shows strong antimicrobial activity against Gram-positive and Gram-negative microorganisms. It inhibits the growth of 99.9% of pathogens within 2 h.[25] Two of the effective characteristics of copper nanoparticles are their small size and high surface area to mass ratio. The exact mechanism is unknown.[26] Accumulation of copper nanoparticles on the cell surface can induce a reduction in membrane integrity and subsequently cause cytoplasmic leakage.[27] When they have crossed the cell membrane, copper nanoparticles can inactivate proteins, and induce DNA damage and apoptosis by interacting with the thiol groups of intracellular proteins.[28] The effect of a combination of nanoparticles opens up a new avenue where the desirable and useful properties of each of the nanoparticles, such as their optical and mechanical properties, can be combined.[29] The antimicrobial properties of both TiO_2 and CuO nanoparticles alone or as composites or coated on surfaces have been reported previously.[30–33] However, limited information is available on the potential antimicrobial activity of $Cu_2Ti_2O_5$ nanoparticles. Therefore, the development of $Cu_2Ti_2O_5$ nanostructures with antimicrobial properties is of considerable interest.

Our research focused on synthesizing $Cu_2Ti_2O_5$ nanoparticles and evaluating their impact on the growth and biofilm formation of *P. aeruginosa* and *K. pneumoniae*, which were isolated from respiratory infections. Additionally, we investigated the potential anticancer properties of these nanoparticles.

2. Materials and methods

2.1. Fabrication of $Cu_2Ti_2O_5$ nanostructures

$Cu_2Ti_2O_5$ nanostructures were prepared by the Pechini method. This synthesis method was achieved by preparing two separate solutions as follows: first, a stoichiometric amount of 0.165 g of copper(II) nitrate trihydrate (Merck, $Cu(NO_3)_2 \cdot 3H_2O$, CAS 10031-43-3) was dissolved in 15 mL of ethyl alcohol (Merck, C_2H_5OH, CAS 64-17-5) as solvent and was denoted solution "A". Then, solution "B" was prepared separately by simultaneously dissolving 0.233 mL of titanium(IV) butoxide (Sigma, $Ti(OBu)_4$, CAS 97 5593-70-4) in 15 mL of ethyl alcohol (cation ratio Ti : Cu = 1 : 1). Then, 0.4 g of citric acid (Merck, $C_6H_8O_7$, CAS 77-92-9) was completely dissolved in 10 mL of ethyl alcohol, added to solution "A" and stirred for 30 min to enhance the complexation process. After that, both solutions "A" and "B" were mixed under vigorous stirring. Then 0.114 mL of ethylene glycol (Sigma, $(CH_2OH)_2$, CAS 107-21-1) was added and heated to 90 °C to obtain a viscous gel. The molar ratio of metal ions to citric acid : ethylene glycol was 1 : 3 : 3. Finally, the viscous gel was placed in an oven at 80 °C to dry, and the dried powder was calcined in an alumina crucible at different temperatures (700 °C (Sample 1), 800 °C (Sample 2), 900 °C (Sample 3)) for 2 h (Scheme 1).

2.2. Characterization of nanoparticles

The structural features and nature of the functional groups associated with the nanoparticles were characterized by Fourier

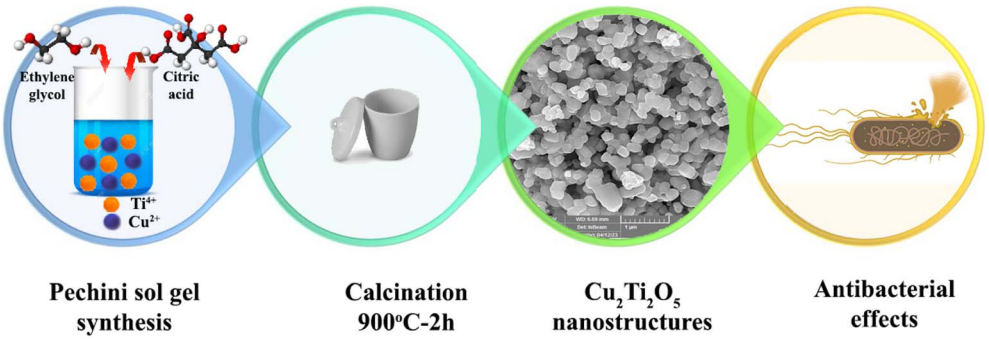

Scheme 1 Schematic fabrication of $Cu_2Ti_2O_5$ as the active material for antibacterial application.

transform infrared spectroscopy (FTIR) in KBr pellets using a Shimadzu Varian 4300 spectrophotometer in the range 400–4000 cm^{-1}. X-ray diffraction (XRD) patterns were obtained using an X′Pert PRO X-ray diffractometer (Philips), sieved through copper Ka irradiation ($\lambda = 15.4$ nm). An energy dispersive X-ray (EDX) analysis device with a 20 kV stimulating charge was used for elemental analysis, determining the electronic state, and chemical characterization. The surface morphology of the nanoparticles was studied through scanning electron microscopy (SEM, LEO-1455VP), and morphological investigation and analysis of particle size distribution were performed with a transmission electron microscope (TEM, Philips EM208S).

2.3. Bacterial strains

Twenty clinical samples of *P. aeruginosa* and *K. pneumoniae* were isolated from patients with respiratory infections, who were hospitalized in Shahid Beheshti Hospital, Kashan, Iran. Additionally, two standard isolates of *Klebsiella pneumoniae* ATCC 10031 and *Pseudomonas aeruginosa* ATCC 27853 (prepared by the Department of Microbiology, Kashan University of Medical Sciences) were selected as reference controls. The clinical isolates were cultured in blood agar, MacConkey agar, and EMB agar media. After 24 h of incubation at 37 °C, suspicious colonies were examined macroscopically and microscopically, and isolates were confirmed *via* Gram staining and standard biochemical tests. Then they were stored in trypticase broth medium and glycerol (70 : 30, respectively) (Merck-Germany) at −70 °C for use in the next steps.

2.4. Determination of MIC and MBC

The microdilution method was used to evaluate the minimum inhibitory concentration (MIC) of titanium copper oxide nanoparticles for both *P. aeruginosa* and *K. pneumoniae*. Serial dilution of nanoparticles was used in a 96-well microtiter plate in the range of 9.7–2500 μg mL^{-1}.

All tests were conducted in Mueller–Hinton broth, followed by mixing of nanoparticles in 20% dimethylsulfoxide (DMSO). 100 μL of Mueller–Hinton broth culture medium were added to a 96-well microtitre plate. Then, 100 μL of nanoparticles were added to the first well and diluted up to well 9, and 100 μL of the ninth well were discarded. Finally, 10 μL of bacterial suspension (dilution 1/20) was added to all the wells except for wells 10 and 12. Similar experiments were conducted for the negative control (100 μL of culture medium) and the positive control (culture medium + bacterial suspension). To ensure the correctness of the experiment, one well was considered as a control substance (only 100 μL of the desired substance). The microplates were then placed in a 37 °C incubator for 24 h. The lowest dilution at which no turbidity was observed was considered the MIC.[34] The lowest concentration of nanoparticles that kills ≥99.9% (3 log) of the bacteria was also determined as the MBC. For this, samples were taken from the wells showing no growth, spread onto nutrient agar plates, and incubated at 35 °C for 24 h. The MBC was determined based on the 3 log decrease in the viable population of the bacteria.[35]

2.5. Determination of inhibition of biofilm formation

2MIC, MIC, and 1/2MIC concentrations of nanoparticles were selected. Firstly, the bacteria were cultured in Luria–Bertani medium for 24 h at 37 °C. After that, fresh Luria–Bertani medium was used to dilute the samples, and the samples cultured in Luria–Bertani were first brought to 0.5 McFarland with fresh Luria–Bertani culture medium and then diluted 1 : 100. 100 μL of nanoparticles in three concentrations of 2MIC, MIC, and 1/2MIC were added to each well. For each nanoparticle concentration, three wells were allocated for each isolate. 100 μL of each diluted sample were added to the wells of a 96-well microplate. For each isolate, three wells were allocated for each concentration and sample, 200 μL of BHI culture medium was used as a negative control, and bacteria plus medium were used as a positive control. The microplate containing the samples was incubated at a temperature of 37 °C for 24 h. Next, the wells were washed once with PBS and dried at room temperature. To fix the samples, 200 μL of methanol was added to the wells for 20 min and allowed to dry at room temperature. Crystal violet (0.2%, 200 μL) was added to the wells for 10 min. The crystal violet dye was washed with distilled water and allowed to dry. 200 μL of 33% acetic acid were added to each well, and 15 min later the absorbance was measured at 570 nm using an ELISA reader. Finally, the biofilm inhibitory percentage was calculated with the following formula:[36] Percentage reduction $= 100 \times ((C - B) - (T - B))/((C - B))$; $C =$ average biofilm formed; $T =$ the average of wells containing bacteria under the effect of nanoparticles; and $B =$ average of wells containing medium.

2.6. Determining the anti-cancer properties of nanoparticles

All the procedures were performed under a Class II laminar flow hood. In the MTT method, to check the cytotoxicity, a suspension containing 100 000 A549 cells per mL (human lung carcinoma epithelial cells) was first prepared. For each 96-well plate, about 9.6 mL of cell suspension was needed. To prevent evaporation of the wells, the required humidity was provided inside the incubator. Each test required at least three replicates and 7–8 control wells.

The suspension was prepared by scraping the cells from the bottom of the flask. The previous culture medium was removed from the flask, and then the cells were separated from the bottom of the flask using trypsin. A milliliter of trypsin was added to the cells and then placed in a 37 °C incubator for 3–5 min, and the cells were separated from the bottom of the flask.

Then, a fresh culture medium containing 8.5 mL of DMEM medium and 1.5 mL of serum was added to the chosen flask. The cells were well separated from the bottom of the well by multiple pipetting. Next, 100 μL of the suspension was added to each well. About 10 000 cells were placed in each well. The plate was placed in 37 °C incubator for 18–24 h. After 24 h, 80% of each well was filled with cells. Then, a two-fold serial dilution of nanoparticles was prepared. 100 μL of each dilution was added to half of the wells. Half of the wells contained 100 μL of culture medium containing cells and 100 μL of nanoparticle dilutions (48 h).

Only a blank medium was added to the control wells. Then the plate was incubated in a 37 °C incubator with 95% humidity and 5% carbon dioxide for 24 h. After 24 h, the nanoparticles were added to the remaining wells with 80% cells in three replicates at the same concentration. After 24 h, the medium inside each well was emptied. 100 μL of the mixture of 10% MTT solution with RPMI medium was added to each well. After mixing, the plate was placed in a 37 °C incubator for 4 h. Then the solution was emptied from the wells and 100 μL of DMSO was added to each well. After combining the cells with DMSO, the cell viability was obtained from a comparison of the absorbance of each sample with the control sample at a wavelength of 570 nm. The percentage of living cells, or the rate of cell survival in the cytotoxicity test, was calculated based on the following formula:[37]

$$\text{Percentage of viable cells} = \text{average absorbance of treated samples/average absorbance of control samples} \times 100.$$

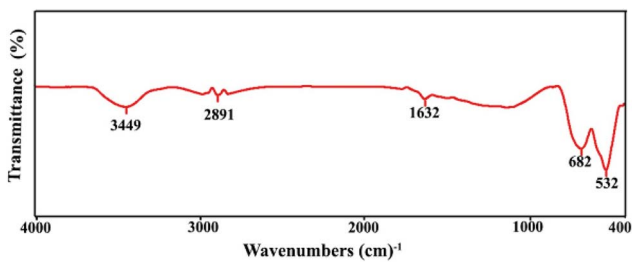

Fig. 1 FTIR spectrum of $Cu_2Ti_2O_5$ nanostructures prepared in the presence of citric acid at 900 °C for 2 h.

3. Results

3.1. *Characteristics of* $Cu_2Ti_2O_5$

3.1.1. FTIR spectrum. The FTIR spectrum of $Cu_2Ti_2O_5$ nanostructures synthesized using the Pechini method at 900 °C for 2 h is presented in Fig. 1. The bands observed at 3449 and 1632 cm^{-1} were related to the stretching and bending vibrations of the O–H groups in the water molecules adsorbed on the surface of the nanoparticles. The FTIR band at the frequency of 2891 cm^{-1} corresponded to the $-CH_2$ stretching vibration of the remaining citric acid.[38] The main typical bands at 682 and 532 cm^{-1} were attributed to the vibrations of Ti–O[30] and Cu–O[39,40] functional groups, respectively.

3.1.2. XRD patterns. X-ray diffraction (XRD) patterns were used to investigate the effect of calcination temperature on the crystallographic structure of the synthesized samples. As shown in Fig. 2a, when the temperature of the calcine was 700 °C (Sample 1), a mixture of two compounds, TiO_2 and CuO with reference codes 01-077-0441 and 01-080-1917, was formed. Sample 2, prepared at a calcination temperature of 800 °C, showed the formation of the $Cu_2Ti_2O_5$ (00-024-0340) structure as the main phase with impurity peaks corresponding to TiO_2 rutile phase (01-077-0441), and TiO_2 anatase phase (00043-1029) (Fig. 2b). In Fig. 2c, all the peak positions in the XRD pattern of Sample 3 (prepared at a calcination temperature of 900 °C) showed the formation of pure $Cu_2Ti_2O_5$ nanoparticles without any impurity peaks.

3.1.3. EDX analysis. The EDX technique was used to check the composition and purity of the optimal sample. As can be seen in Fig. 3, the presence of Cu, Ti, and O elements with the

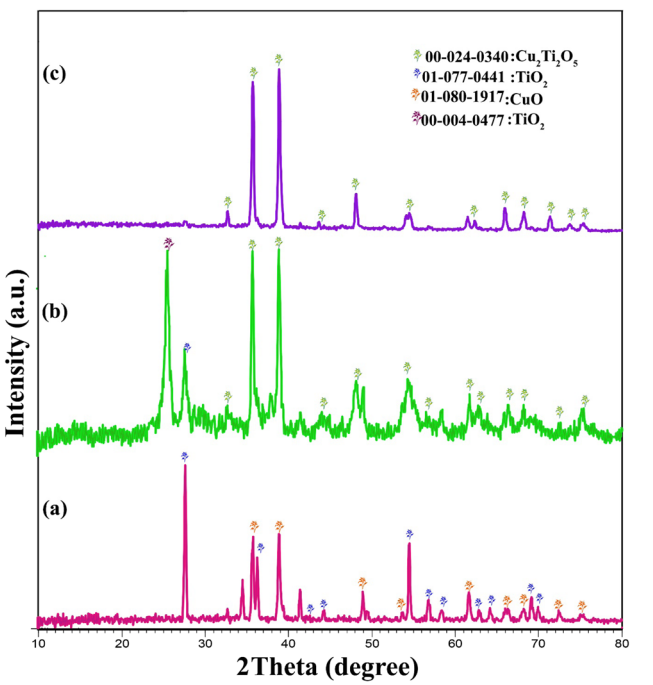

Fig. 2 XRD patterns of $Cu_2Ti_2O_5$ nanostructures prepared in the presence of citric acid: (a) Sample 1 (b) Sample 2, and (c) Sample 3.

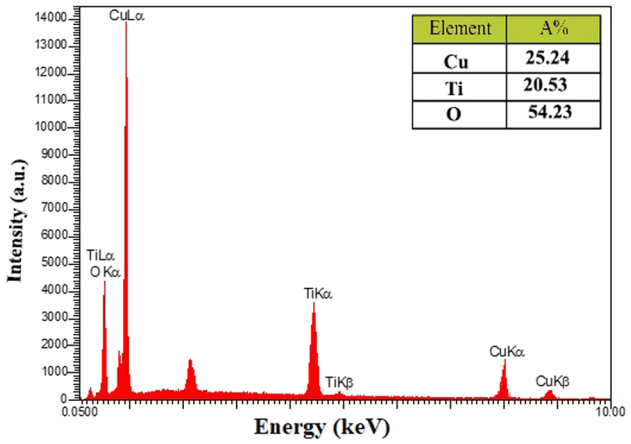

Fig. 3 EDS spectrum of $Cu_2Ti_2O_5$ nanostructures, prepared in the presence of citric acid at 900 °C for 2 h.

expected stoichiometric ratio was strong evidence for the successful synthesis of $Cu_2Ti_2O_5$ nanoparticles.

3.1.4. Results for FESEM and TEM. One of the main problems in the way of developing nanoscale products is trying to achieve a product with special characteristics and precise control over the morphology. The Pechini method is considered a very favorable process for the synthesis of alkaline-earth titanates and niobates. In the flexible approach of the Pechini method, solutions of metal salts and citric acid together were used to prepare cationic metal complexes. At a temperature of 150 °C, the carboxylic groups of these complexes and hydroxyl groups of ethylene glycol participated in the transesterification reaction, and an internal polymer gel network was formed. Uniformity and phase segregation were achieved by the dispersion of raw materials in the polymer matrix. Finally, by heating the gel at a high temperature, an oxide product was formed. In this experimental work, the Pechini approach was used for the first time for the synthesis of $Cu_2Ti_2O_5$ nanostructures. For this purpose, SEM spectroscopy was used to examine the morphology and particle size of the optimal sample. Fig. 4a and b show SEM images of $Cu_2Ti_2O_5$ nanostructures in the form of irregular polyhedral microstructures. The particle size distribution plot produced using Digimizer gave an optimal average sample size of 118.91 nm (Fig. 4c). The results confirmed that metal ions in the presence of citric acid as a chelating agent together with ethylene glycol create

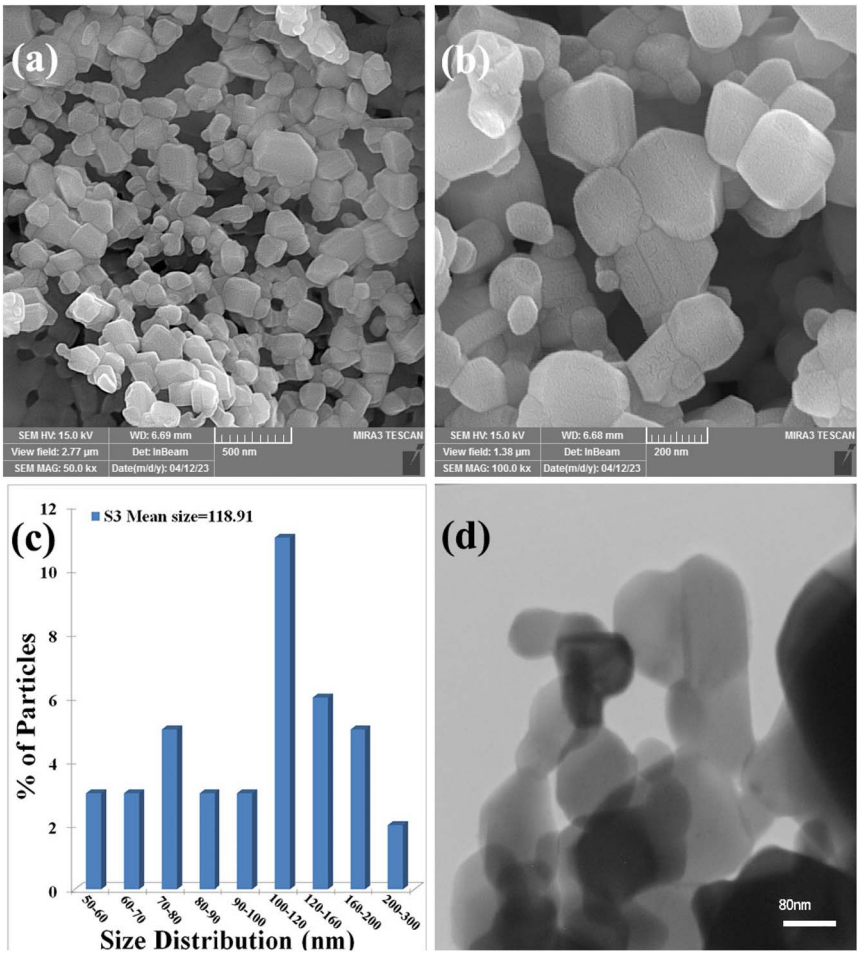

Fig. 4 (a and b) FESEM micrographs of $Cu_2Ti_2O_5$ nanomaterials prepared in the presence of citric acid at 900 °C for 2 h. (c) Size distribution diagram estimated by Digimizer software of Sample 3. (d) TEM image of $Cu_2Ti_2O_5$ nanostructures.

Table 1 Determination of MIC value (μg mL^{-1}) and MBC value (μg mL^{-1}) for clinical and standard isolates of *K. pneumonia*

Bacteria	MIC	MBC
K. pneumoniae	625–156.25 μg mL^{-1}	625 μg mL^{-1}
K. pneumoniae ATCC 10031	156.25 μg mL^{-1}	312.5 μg mL^{-1}
P. aeruginosa	1250–625 μg mL^{-1}	1250 μg mL^{-1}
P. aeruginosa ATCC 27853	78.125 μg mL^{-1}	312.5 μg mL^{-1}

a homogeneous polymer network and as a result a suitable clustering of nanoparticles. To further investigate the morphology of the products, TEM images of $Cu_2Ti_2O_5$ nanostructures are shown in Fig. 4d. In Fig. 4d, it can be seen that nanostructures containing irregular polyhedral shapes were produced. In addition, the presence of suitably clustered particles was confirmed by TEM images.

3.2. Antibacterial activity

3.2.1. Determination of the MICs and MBCs. As shown in Table 1 and Fig. 5, the MIC values of $Cu_2Ti_2O_5$ against the *K. pneumoniae* isolates ranged from 156.25 to 625 μg mL^{-1}, and for *P. aeruginosa* ranged from 625 to 1250 μg mL^{-1}. MBC is the lowest concentration of antibacterial agent to kill bacteria (showing no growth on an agar plate). The MBC for *K. pneumoniae* was 625 μg mL^{-1}, while *P. aeruginosa* showed an MBC value of 1250 μg mL^{-1}. The MIC and MBC values for *P. aeruginosa* showed that *P. aeruginosa* was less susceptible to $Cu_2Ti_2O_5$.

3.2.2. Inhibition of biofilm formation. Most *K. pneumoniae* isolates (80%) produced (37.5% weak, 25% moderate, and 37.5% strong) biofilm in BHI broth containing 1% (w/v) sucrose (Table 2), while most *P. aeruginosa* isolates (90%) produced (55.5% weak, and 44.5% strong) biofilm (Table 3). $Cu_2Ti_2O_5$ demonstrated a reduction in biofilm formation in clinical isolates of *P. aeruginosa* and *K. pneumoniae*. The average reductions were 86% and 89% at 2MIC, 74% and 78% at MIC, and 53% and 54% at 1/2MIC concentrations, with no statistically significant differences observed between the results (P value > 0.05) (Fig. 6a). The results of the effects of $Cu_2Ti_2O_5$ nanoparticles on biofilm formation in standard isolates are also shown in Fig. 6b. $Cu_2Ti_2O_5$ at the determined MIC concentration completely inhibited biofilm formation in 25% (2 out of 8) *K. pneumoniae* isolates and 11.1% (1 out of 9) *P. aeruginosa* isolates. Additionally, in 75% (6 out of 8) of *K. pneumoniae* isolates and 55.5% (5 out of 9) of *P. aeruginosa* isolates, the optical density significantly reduced biofilm formation from moderate or strong to weak. In culture media that contained a sub-MIC of $Cu_2Ti_2O_5$, a reduction in biofilm formation was observed in 75% of *K. pneumoniae* isolates and 44.4% of *P. aeruginosa* isolates; none of the *K. pneumoniae* and *P. aeruginosa* isolates showed full inhibition of biofilm formation at this concentration of $Cu_2Ti_2O_5$. Our results showed that the effect of $Cu_2Ti_2O_5$ was much greater for isolates with strong biofilm compared to isolates with weak biofilm.

3.3. Determining the anti-cancer activity of nanoparticles

The MTT test was used to determine the impact of $Cu_2Ti_2O_5$ nanoparticles on the proliferation of A549 cancer cells taken from lung cancer tissue. During this process, cancer cells that filled 80% of each well (Fig. 7a) were treated with $Cu_2Ti_2O_5$ nanoparticles for 24 and 48 h at various concentrations ranging from 1.875 to 1000 μg mL^{-1} (Fig. 7b). $Cu_2Ti_2O_5$ nanoparticles at concentrations of 150–200 μg mL^{-1} and 30–40 μg mL^{-1} cause

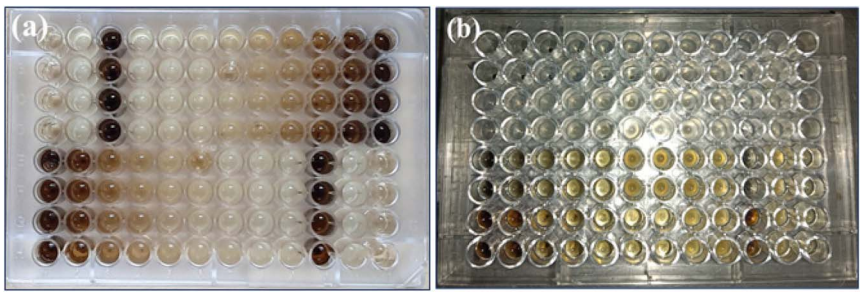

Fig. 5 Determining the minimum inhibitory concentration of $Cu_2Ti_2O_5$ nanoparticles for clinical isolates of *K. pneumoniae* and *P. aeruginosa* (a) and standard isolates of *K. pneumoniae* ATCC 10031 and *P. aeruginosa* ATCC 27853. (b) Repeated twice by the microdilution broth method.

Table 2 The effect of $Cu_2Ti_2O_5$ nanoparticles on biofilm formation of *K. pneumoniae* strains

		Treatment with 2MIC of $Cu_2Ti_2O_5$-NP		Treatment with MIC of $Cu_2Ti_2O_5$		Treatment with sub-MIC of $Cu_2Ti_2O_5$-NP		
Biofilm	No $Cu_2Ti_2O_5$-NP	No biofilm	Weak	No biofilm	Weak	No biofilm	Weak	Moderate
Weak	3 (37.5%)	2 (66.6%)	1 (33.4%)	1 (33.4)	2 (66.6%)	—	3 (100%)	—
Moderate	2 (25%)	1 (50%)	1 (50%)	1 (50%)	1 (50%)	—	2 (100%)	—
Strong	3 (37.5%)	1 (33.4%)	2 (66.6%)	—	3 (100%)	—	1 (33.3%)	2 (66.7%)
Total	8	4 (50%)	4 (50%)	2 (25%)	6 (75%)	—	6 (75%)	2 (25%)

Table 3 The effect of $Cu_2Ti_2O_5$ nanoparticles on the biofilm formation of *P. aeruginosa* strains

		Treatment with 2MIC of $Cu_2Ti_2O_5$-NP		Treatment with MIC of $Cu_2Ti_2O_5$			Treatment with sub-MIC of $Cu_2Ti_2O_5$-NP		
Biofilm	No $Cu_2Ti_2O_5$-NP	No biofilm	Weak	No biofilm	Weak	Moderate	No biofilm	Weak	Moderate
Weak	5 (55.5%)	2 (40%)	3 (60%)	1 (20%)	3 (60%)	1 (20%)	—	3 (60%)	2 (40%)
Moderate	—	—	—	—	—	—	—	—	—
Strong	4 (44.5%)	1 (25%)	3 (75%)	—	2 (50%)	2 (50%)	—	1 (25%)	3 (75%)
Total	9	3 (33%)	6 (66.6%)	1 (11.1%)	5 (55.5%)	3 (33.3%)	—	4 (44.4%)	5 (55.6%)

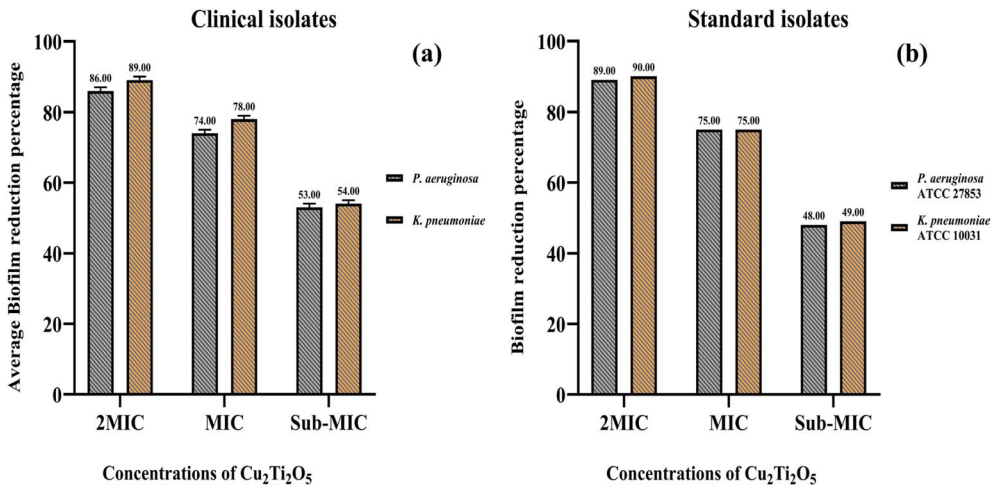

Fig. 6 Comparison of the effects of $Cu_2Ti_2O_5$ nanoparticles on biofilm formation of (a) clinical isolates (*P* value > 0.05) and (b) standard isolates of *Pseudomonas aeruginosa* and *Klebsiella pneumonia*.

50% death of a549 cancer cells (IC50) in 24 and 48 h, respectively (Fig. 8). These findings indicated that the effect of the nanoparticles on the growth of lung cancer cells was more obvious during the first 24 h of treatment. The results suggested that $Cu_2Ti_2O_5$ nanoparticles could be promising anti-cancer agents to inhibit the proliferation of lung cancer cells.

4. Discussion

Hospital-acquired pneumonia (HAP) is one type of hospital-acquired infection that most frequently results in death.[41] Two of the most important pathogens that cause HAP are *K. pneumoniae* and *P. aeruginosa*, which, with the formation of biofilms, cause patients to stay in hospital for a long time and increase patient mortality and significant costs for healthcare providers.[6,42] The spread of antibiotic resistance and the emergence of resistant pathogens has increased interest in alternative therapeutic strategies. One alternative strategy is the use of metal nanoparticles, whose potential effects have been observed on bacterial isolates.[43] In this research, $Cu_2Ti_2O_5$ nanoparticles were synthesized for the first time by the Pechini method, and the XRD results showed the formation of peaks in Sample 3 (900 °C), which confirmed the purity of the $Cu_2Ti_2O_5$ nanoparticles. According to SEM, the $Cu_2Ti_2O_5$ nanoparticles

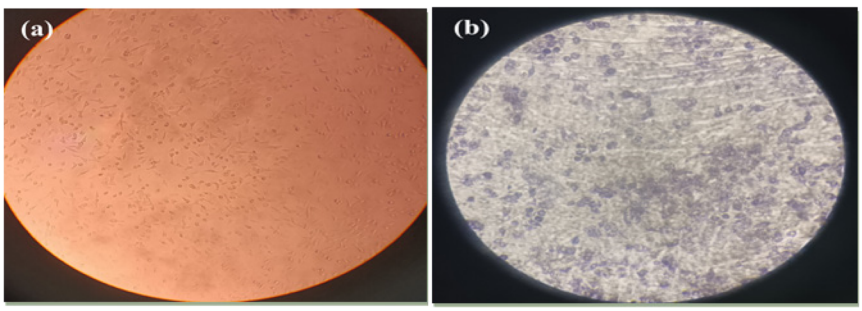

Fig. 7 (a) Microscopic images of the A549 cell line, showing the cells in the well that have filled 80% and are considered as a control. (b) The effect of nanoparticles on the cancer cells following the MTT assay, which caused a reduction in the proliferation of cancer cells.

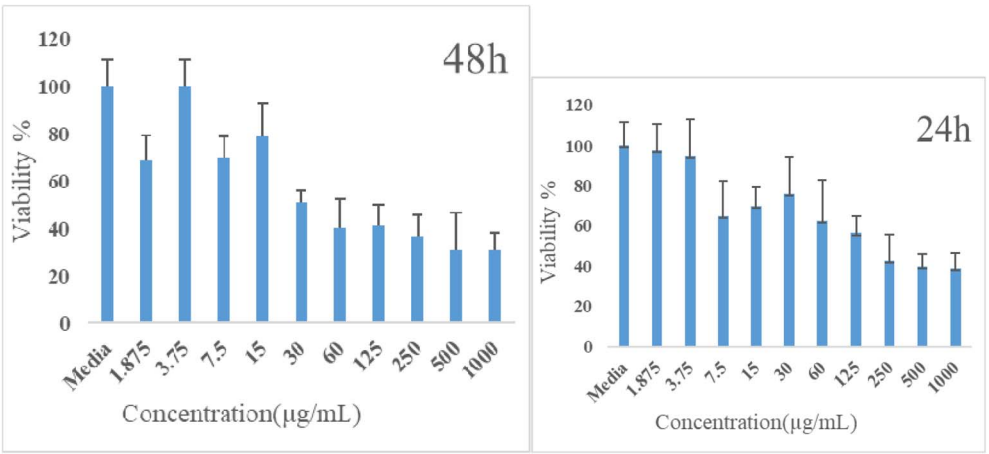

Fig. 8 MTT tests demonstrated that $Cu_2Ti_2O_5$ nanoparticles had an *in vitro* cytotoxicity effect on A549 cancer cells, after 24 h, IC50 concentrations were 150 to 200 μg mL^{-1} against A549, and after 48 h, IC50 concentrations were 30 to 40 μg mL^{-1}. Three experiments were used to express the data using mean ± SD, and cytotoxicity (%) was expressed as compared to untreated controls (*$P < 0.05$).

have an irregular polyhedral form with an average size of 118.91 nm, consistent with research by Valian *et al.* in 2022. In that study, a nanocomposite of chitosan and $Ho_2Ti_2O_7$ was synthesized using the sol–gel auto combustion method with a size of 30 to 60 nm.[44] In our study, ethylene glycol was used as a hydroxyl group donor, and citric acid as a chelating agent.

Several studies indicated that TiO_2 and CuO nanoparticles exhibited antibacterial activity against *K. pneumoniae* and *P. aeruginosa* (Table 4).[45–47] In this study, it was found that $Cu_2Ti_2O_5$ nanoparticles hindered the growth of *P. aeruginosa* and *K. pneumoniae* at concentrations ranging from 625 to 1250 μg mL^{-1} and 156.20 to 625 μg mL^{-1}, respectively. The MIC for *K. pneumoniae* ATCC 10031 and *P. aeruginosa* ATCC 27853 were determined to be 78.125 and 156.25 μg mL^{-1}, respectively. A study conducted by Moorthy Maruthapandi *et al.* in 2020 reported that TiO_2 and CuO nanoparticles did not have any significant antibacterial effects on standard isolates of *P. aeruginosa* PAO1 or *K. pneumoniae* ATCC 700603. However, when they were combined with PANI (TiO_2-PANI, CuO-PANI), their antibacterial effects were enhanced, inhibiting the growth of these bacteria at a concentration of 1 mg mL^{-1}.[47] The difference in the antibacterial effects may be attributed to the different methods used to determine MIC in the two studies. The agar dilution method was used in Moorthy Maruthapandi's study, while the broth microdilution method was used in our study. Additionally, the difference in the isolates used may have contributed to the variation in results. In our study, Cu_2TiO_5 nanoparticles inhibited the growth of *K. pneumoniae* ATCC 10031 and *Pseudomonas aeruginosa* ATCC 27853 at MIC concentrations of 78.125 and 156.25 μg mL^{-1}. A study conducted by Sabar Jabbar Shawkat *et al.* in 2021 revealed that TiO_2 nanoparticles had inhibitory effects at concentrations of 1.208 and 1.166 mg mL^{-1} against *P. aeruginosa* and *K. pneumoniae* isolated from urinary tract infections,[48] which were consistent with our findings.

In a study conducted by Fatma Y Ahmed *et al.* in 2020, it was found that TiO_2 nanoparticles at concentrations ranging from 8 to 64 μg mL^{-1} were able to inhibit the growth of *Pseudomonas aeruginosa*. This significant difference in the MIC results may be due to the size of the nanoparticles (the size of the TiO_2 synthesized in their study was 64.77 nm), but in our study, the average size of the $Cu_2Ti_2O_5$ nanoparticles was 118.91 nm. The size of the nanoparticles is important because the smaller size of the nanoparticles improves interactions with the bacterial cell surface and strengthens their antibacterial effects. However, it is important to note that the clinical samples in Fatma Y Ahmed *et al.*'s study consisted mostly of non-respiratory infections (24 out of 25 isolates) and were not related to hospital-acquired respiratory infections, which may be different in response and resistance to nanoparticles.[49]

The formation of biofilm related to *Pseudomonas aeruginosa* and *Klebsiella pneumoniae* contributes significantly to the spread of antibiotic resistance and infection caused by these bacteria.[50,51] In the present study, it was shown that $Cu_2Ti_2O_5$ nanoparticles have a significant impact on the formation of biofilms by *K. pneumoniae* and *P. aeruginosa*. $Cu_2Ti_2O_5$ nanoparticles at MIC concentration completely inhibited biofilm formation in 25% of *K. pneumoniae* and 11.1% of *P. aeruginosa*. In 75% of *K. pneumoniae* and 44.4% of *P. aeruginosa*, it had reduced strong and medium biofilm to weak biofilm. A study conducted by Sabar Jabbar Shawkat *et al.* in 2021 reported that TiO_2 at a concentration of 1.568 mg mL^{-1} reduced biofilm formation by *Pseudomonas aeruginosa* PTCC 1690 by 21% and *K. pneumoniae* PTCC 1290 by 48%.[48] The difference between the results of that study and our study may be due to the type of samples collected, as in our study, isolates related to HAP were collected, but in Sabar Jabbar Shawkat's study, standard isolates were used. Also, $Cu_2Ti_2O_5$ nanoparticles probably have greater ability to interact with and penetrate bacterial cells and inhibit biofilm formation due to their polygonal shape and dimensions.

Another study conducted by Minha Naseer *et al.* showed that CuO synthesized with *Cassia fistula* extract inhibited *K. pneumoniae* biofilm formation by 99.8%. The difference in the

Table 4 Studies that have been conducted on the antibacterial, antibiofilm, and anticancer properties of copper and titanium nanoparticles

Nanoparticles	Size of nanoparticles	Properties	References
Nanocomposite of chitosan and $Ho_2Ti_2O_7$	30 to 60 nm	Synthesis by sol–gel method	44
TiO_2-PANI and CuO-PANI nanoparticles	5 μm	These nanoparticles inhibited the growth of *P. aeruginosa* PAO1 and *K. pneumoniae* ATCC 700603 in the agar dilution method at a concentration of 1 mg ML^{-1}	47
TiO_2 nanoparticles	10 to 25 nm	TiO_2 nanoparticles had inhibitory effects at concentrations of 1.208 and 1.166 mg mL^{-1} against *P. aeruginosa* and *K. pneumoniae* isolated from urinary tract infections	48
TiO_2 nanoparticles	64.77 nm	TiO_2 nanoparticles at concentrations of 8 and 64 μg mL^{-1} inhibited the growth of *P. aeruginosa* isolated from non-respiratory infections	49
TiO_2 nanoparticles	10 to 25 nm	TiO_2 at a concentration of 1.568 mg mL^{-1} reduced biofilm formation by *P. aeruginosa* PTCC 1690 by 21% and *K. pneumoniae* PTCC 1290 by 48%	48
CuO synthesized with *Cassia fistula* extract	43.8 nm	CuO synthesized with *Cassia fistula* extract inhibited *K. pneumoniae* biofilm formation by 99.8%	52
CuO nanoparticles synthesized with *Moringa oleifera*	90 to 250 nm	CuO nanoparticles synthesized with *Moringa oleifera* at a concentration of 1000 μg mL^{-1} inhibited the formation of *K. pneumoniae* by 92%	54
TiO_2 synthesized with *Aloe barbadensis*	20 nm	TiO_2 synthesized with *Aloe barbadensis* Mill. Inhibited biofilm formation by 47.04% in *K. pneumoniae* MTCC 2453	60
TiO_2 nanoparticles synthesized with *Cynodon dactylon*	13 to 34 nm	TiO_2 nanoparticles synthesized with *Cynodon dactylon* had IC50 of 140 to 200 μg mL^{-1} for the A549 cell line	55
Zinc oxide doped TiO_2 nanocrystals	5 to 50 nm	Zinc oxide nanoparticles and TiO_2 crystals had IC50 of 170 μg mL^{-1} for the A549 cell line	56
TiO_2 nanoparticles	10 to 25 nm	TiO_2 inhibited MCF-7 growth by 41.30 and 56.33% at concentrations of 170 and 200 μg mL^{-1} in 48 h	57
TiO_2 nanoparticles	15.5 to 169.5 nm	No significant inhibition was observed when V79 Chinese hamster lung fibroblast cells were exposed to concentrations up to 400 ppm TiO_2	58

results may be due to the difference in the isolates used. In the study by Minha Naseer *et al.*, a single *K. pneumoniae* isolate was identified from non-hospital-acquired pneumonia.[52] However, in our study, 10 isolates were recovered from hospital-acquired respiratory infections, which may show differences in resistance factors and the strength of biofilm formation.

The difference in the size and shape of nanoparticles may also be effective in inhibiting biofilm formation.[53] In a study carried out by Boliang Bai *et al.* in 2022, it was reported that CuO nanoparticles synthesized with *Moringa oleifera* with dimensions of 90 to 250 nm at a concentration of 1000 μg mL^{-1} inhibited the formation of *K. pneumoniae* by 92%.[54] In 2019, J. Rajkumari *et al.* showed that TiO_2 synthesized with *Aloe barbadensis* Mill. with an average size of 20 nm and relatively spherical shape inhibited biofilm formation by 47.04% in *K. pneumoniae* MTCC 2453.[60]

Several studies have been conducted on the anticancer effects of nanoparticles (Table 4). In the present study, the anticancer effects of $Cu_2Ti_2O_5$ nanoparticles were measured by an MTT test, and it was observed that $Cu_2Ti_2O_5$ in concentrations of 150 to 200 μg mL^{-1} and 30 to 40 μg mL^{-1} at 24 and 48 h caused the death of 50% of A549 cancer cells (IC50), which was consistent with studies conducted by Hariharan *et al.* in 2017 and K. Kaviyarasu *et al.* in 2017. In the study by Hariharan *et al.* in 2017, it was reported that TiO_2 nanoparticles synthesized with *Cynodon dactylon* had an IC50 of 140 to 200 μg mL^{-1} for the A549 cell line.[55] In the study by K. Kaviyarasu *et al.*, it was reported that zinc oxide nanoparticles and TiO_2 crystals had an IC50 of 170 μg mL^{-1} for the A549 cell line.[56] In another study, Hoda Lothian reported that TiO_2 did not show any significant effect on MCF-7 at 24 h, but in 48 h, at concentrations of 170 and 200 μg mL^{-1}, it inhibited MCF-7 growth by 41.30% and 56.33%, respectively.[57] Keith B. Male *et al.* reported that no significant toxicity/inhibition was observed when V79 Chinese hamster lung fibroblast cells were exposed to concentrations up to 400 ppm of TiO_2.[58] The results obtained from the present study on the A549 cell line indicated the significant effects of $Cu_2Ti_2O_5$ on inhibiting the growth of cancer cells, which may be

due to the small size of the nanoparticles and their polygonal shape, which improved their surface reactivity.[59]

The findings of this study showed that $Cu_2Ti_2O_5$ nanoparticles have the potential to prevent the growth of cancer cells and also to suppress biofilm growth in both *K. pneumoniae* and *P. aeruginosa* isolates. However, further research is necessary to determine the effects of these nanoparticles in *in vivo* conditions.

5. Conclusions

$Cu_2Ti_2O_5$ nanoparticles were successfully synthesized for the first time using the Pechini method. Their characteristics were investigated using XRD, FTIR, SEM, TEM, and EDX analysis. The antibacterial and antibiofilm effects of $Cu_2Ti_2O_5$ were evaluated, and it was discovered that it has the ability to control hospital-acquired pneumonia infections associated with *K. pneumoniae* and *P. aeruginosa.* $Cu_2Ti_2O_5$ was also found to have significant effects in inhibiting the growth of A549 lung cancer cells. However, for the use of this nanoparticle in clinical applications, including ventilators and hospital environments, its effects on more isolates and in *in vivo* conditions, and the stability of the nanoparticle in the environment need to be investigated.

Ethics statement

The present study has received ethical approval from the Ethics Committee of Kashan University of Medical Sciences in Iran (IR.KAUMS.MEDNT.REC.1402.263).

Data availability

The authors confirm that the data supporting the findings of this study are available within the article. Additional data are available from the corresponding author upon reasonable request.

Conflicts of interest

The authors declare that they have no known competing financial interests or personal relationships that could have appeared to influence the work reported in this paper.

Acknowledgements

The authors are grateful to the council of Iran National Science Foundation (INSF: 97017837) and the University of Kashan, Grant No. (159271/MP1) for supporting this work. This study was financially supported by the Vice-Chancellor of Research, Kashan University of Medical Sciences, Kashan, Iran (Grant No. 402167).

References

1 S. Raoofi, F. Pashazadeh Kan, S. Rafiei, Z. Hosseinipalangi, Z. Noorani Mejareh, S. Khani, B. Abdollahi, F. Seyghalani Talab, M. Sanaei and F. Zarabi, *PLoS One*, 2023, **18**, e0274248.
2 H. A. Khan, A. Ahmad and R. Mehboob, *Asian Pac. J. Trop. Biomed.*, 2015, **5**, 509–514.
3 K. H. P. Riwu, M. H. Effendi, F. A. Rantam, A. R. Khairullah and A. Widodo, *Vet. World*, 2022, **15**, 2172.
4 M. Imran, A. Amjad and F. R. Haidri, *Pak. J. Med. Sci.*, 2016, **32**, 823.
5 S. Morris and E. Cerceo, *Antibiotics*, 2020, **9**, 196.
6 S.-S. Jean, Y.-C. Chang, W.-C. Lin, W.-S. Lee, P.-R. Hsueh and C.-W. Hsu, *J. Clin. Med.*, 2020, **9**, 275.
7 M. Assefa and A. Amare, *Infect. Drug Resist.*, 2022, 5061–5068.
8 S. T. Micek, R. G. Wunderink, M. H. Kollef, C. Chen, J. Rello, J. Chastre, M. Antonelli, T. Welte, B. Clair and H. Ostermann, *Crit. Care*, 2015, **19**, 1–8.
9 N. Sathe, P. Beech, L. Croft, C. Suphioglu, A. Kapat and E. Athan, *Infect. Med.*, 2023, **2**, 178–194.
10 M. Esmaeilnia, M. Saffari, S. Rashki, Z. Marzhoseyni, A. Khaledi, G. A. Moosavi, F. Atoof and B. Alani, *Iran. J. Basic Med. Sci.*, 2022, **25**, 208.
11 F. Giovagnorio, A. De Vito, G. Madeddu, S. G. Parisi and N. Geremia, *Antibiotics*, 2023, **12**, 1621.
12 S. Sharma, V. Kaushik and V. Tiwari, in *Understanding Microbial Biofilms*, Elsevier, 2023, pp. 209–245.
13 S. Datta, S. Nag and D. N. Roy, *Curr. Med. Res. Opin.*, 2024, 1–20.
14 D. Esmaeili, S. F. Daymad, A. Neshani, S. Rashki, Z. Marzhoseyni and A. Khaledi, *Gene Rep.*, 2019, **16**, 100460.
15 H. Karballaei Mirzahosseini, M. Hadadi-Fishani, K. Morshedi and A. Khaledi, *Microb. Drug Resist.*, 2020, **26**, 815–824.
16 S. M. J. Hosseini, N. S. Naeini, A. Khaledi, S. F. Daymad and D. Esmaeili, *Open Microbiol. J.*, 2016, **10**, 188.
17 G. Mi, D. Shi, M. Wang and T. J. Webster, *Adv. Healthcare Mater.*, 2018, **7**, 1800103.
18 M. Thambirajoo, M. Maarof, Y. Lokanathan, H. Katas, N. F. Ghazalli, Y. Tabata and M. B. Fauzi, *Antibiotics*, 2021, **10**, 1338.
19 E. Hoseinzadeh, P. Makhdoumi, P. Taha, H. Hossini, J. Stelling, M. Amjad Kamal and G. Md Ashraf, *Curr. Drug Metab.*, 2017, **18**, 120–128.
20 G. R. Rudramurthy, M. K. Swamy, U. R. Sinniah and A. Ghasemzadeh, *Molecules*, 2016, **21**, 836.
21 B. Mubeen, A. N. Ansar, R. Rasool, I. Ullah, S. S. Imam, S. Alshehri, M. M. Ghoneim, S. I. Alzarea, M. S. Nadeem and I. Kazmi, *Antibiotics*, 2021, **10**, 1473.
22 L. Chen, J. M. Mccrate, J. C. Lee and H. Li, *J. Nanotechnol.*, 2011, **22**, 105708.
23 A. Laganà, G. Visalli, F. Corpina, M. Ferlazzo, A. Di Pietro and A. Facciolà, *Eur. Rev. Med. Pharmacol. Sci.*, 2023, **27**, 3645–3663.
24 A. B. Younis, Y. Haddad, L. Kosaristanova and K. Smerkova, *Wiley Interdiscip. Rev.:Nanomed. Nanobiotechnol.*, 2023, **15**, e1860.
25 A. M. Shehabeldine, B. H. Amin, F. A. Hagras, A. A. Ramadan, M. R. Kamel, M. A. Ahmed, K. H. Atia and S. S. Salem, *Appl. Biochem. Biotechnol.*, 2023, **195**, 467–485.
26 C. Ashajyothi, K. H. Harish, N. Dubey and R. K. Chandrakanth, *J. Nanostruct. Chem.*, 2016, **6**, 329–341.

27 T. Ameh and C. M. Sayes, *Environ. Toxicol. Pharmacol.*, 2019, **71**, 103220.
28 J. V. M. Zoccal, F. O. Arouca and J. A. S. Gonçalves, *Mater. Sci. Forum*, 2010, **660**, 385–390.
29 M. S. Hassan, T. Amna, H. Y. Kim and M.-S. Khil, *Composites, Part B*, 2013, **45**, 904–910.
30 M. M. Imani, M. Kiani, F. Rezaei, R. Souri and M. Safaei, *Ceram. Int.*, 2021, **47**, 33398–33404.
31 S. Pal, S. Villani, A. Mansi, A. M. Marcelloni, A. Chiominto, I. Amori, A. R. Proietto, M. Calcagnile, P. Alifano and S. Bagheri, *ACS Omega*, 2024, **9**, 45376–45385.
32 A. M. Kumar, A. Khan, R. Suleiman, M. Qamar, S. Saravanan and H. Dafalla, *Prog. Org. Coat.*, 2018, **114**, 9–18.
33 S. Naz, A. Gul, M. Zia and R. Javed, *Appl. Microbiol. Biotechnol.*, 2023, **107**, 1039–1061.
34 P. Spigaglia, F. Barbanti, E. Castagnola, M. C. Diana, L. Pescetto and R. Bandettini, *Anaerobe*, 2017, **48**, 262–268.
35 P. Parvekar, J. Palaskar, S. Metgud, R. Maria and S. Dutta, *Biomater. Invest. Dent.*, 2020, **7**, 105–109.
36 M. M. Sopirala, J. E. Mangino, W. A. Gebreyes, B. Biller, T. Bannerman, J.-M. Balada-Llasat and P. Pancholi, *Antimicrob. Agents Chemother.*, 2010, **54**, 4678–4683.
37 H. Madanchi, S. Akbari, A. A. Shabani, S. Sardari, Y. Farmahini Farahani, G. Ghavami and R. Ebrahimi Kiasari, *Drug Dev. Res.*, 2019, **80**, 162–170.
38 S. Khan, Z. H. Shah, S. Riaz, N. Ahmad, S. Islam, M. A. Raza and S. Naseem, *Ceram. Int.*, 2020, **46**, 10942–10951.
39 M. Valian, M. Masjedi-Arani and M. Salavati-Niasari, *Fuel*, 2021, **306**, 121638.
40 M. A. Haque, M. K. Hossain, M. A. I. Molla, M. Sarker, S. C. Dey and M. Ashaduzzaman, *J. CleanWAS*, 2021, **5**, 27–30.
41 H. Shu, L. Li, Y. Wang, Y. Guo, C. Wang, C. Yang, L. Gu and B. Cao, *Infect. Drug Resist.*, 2020, 4147–4154.
42 S. Baidya, S. Sharma, S. K. Mishra, H. P. Kattel, K. Parajuli and J. B. Sherchand, *BioMed Res. Int.*, 2021, **2021**, 8817700.
43 N. K. Dhami, A. Mukherjee and M. S. Reddy, *Ecol. Eng.*, 2016, **94**, 443–454.
44 M. Valian, M. Salavati-Niasari, S. H. Ganduh, W. K. Abdulsahib, M. A. Mahdi and L. S. Jasim, *Int. J. Hydrogen Energy*, 2022, **47**, 21146–21159.
45 S. Arya, H. Sonawane, S. Math, P. Tambade, M. Chaskar and D. Shinde, *Int. Nano Lett.*, 2021, **11**, 35–42.
46 P. Maheswari, S. Ponnusamy, S. Harish, M. Ganesh and Y. Hayakawa, *Arabian J. Chem.*, 2020, **13**, 3484–3497.
47 M. Maruthapandi, A. Saravanan, J. H. Luong and A. Gedanken, *J. Funct. Biomater.*, 2020, **11**, 59.
48 S. J. Shawkat and K. Chehri, *Avicenna J. Clin. Microbiol. Infect.*, 2021, **8**, 123–129.
49 F. Y. Ahmed, U. Farghaly Aly, R. M. Abd El-Baky and N. G. Waly, *Int. J. Nanomed.*, 2020, 3393–3404.
50 C. Vuotto, F. Longo, M. P. Balice, G. Donelli and P. E. Varaldo, *Pathog. Dis.*, 2014, **3**, 743–758.
51 M. Wu and X. Li, in *Molecular Medical Microbiology*, Elsevier, 2015, pp. 1547–1564.
52 M. Naseer, R. Ramadan, J. Xing and N. A. Samak, *Int. Biodeterior. Biodegrad.*, 2021, **159**, 105201.
53 J. Borcherding, J. Baltrusaitis, H. Chen, L. Stebounova, C.-M. Wu, G. Rubasinghege, I. A. Mudunkotuwa, J. C. Caraballo, J. Zabner and V. H. Grassian, *Environ. Sci.:Nano*, 2014, **1**, 123–132.
54 B. Bai, S. Saranya, V. Dheepaasri, S. Muniasamy, N. S. Alharbi, B. Selvaraj, V. S. Undal and B. M. Gnanamangai, *J. King Saud Univ., Sci.*, 2022, **34**, 102120.
55 D. Hariharan, K. Srinivasan, L. Nehru and J. Nanomed, *Res*, 2017, **5**, 138–142.
56 K. Kaviyarasu, N. Geetha, K. Kanimozhi, C. M. Magdalane, S. Sivaranjani, A. Ayeshamariam, J. Kennedy and M. Maaza, *Mater. Sci. Eng., C*, 2017, **74**, 325–333.
57 H. Lotfian and F. Nemati, *IIOAB J.*, 2016, **7**, 219–224.
58 K. B. Male, M. Hamzeh, J. Montes, A. C. Leung and J. H. Luong, *Anal. Chim. Acta*, 2013, **777**, 78–85.
59 K. S. Tan and K. Y. Cheong, *J. Nanopart. Res.*, 2013, **15**, 1–29.
60 J. Rajkumari, C. M. Magdalane, B. Siddhardha, J. Madhavan, G. Ramalingam, N. A. Al-Dhabi, M. V. Arasu, A. Ghilan, V. Duraipandiayan and K. Kaviyarasu, *J. Photochem. Photobiol., B*, 2019, **201**, 111667.